Environmental Science & Technology

Article

pubs.acs.org/est

Influence of Functional Groups on Organic Aerosol Cloud Condensation Nucleus Activity

Sarah R. Suda,[†] Markus D. Petters,*[,†] Geoffrey K. Yeh,[‡,¶] Christen Strollo,[‡,∥] Aiko Matsunaga,[‡,⊥] Annelise Faulhaber,[‡] Paul J. Ziemann,[‡,@] Anthony J. Prenni,[§,▽] Christian M. Carrico,[§,#] Ryan C. Sullivan,[§,●] and Sonia M. Kreidenweis[§]

[†]Department of Marine Earth and Atmospheric Sciences, North Carolina State University, Raleigh, North Carolina 27695-8208, United States

[‡]Air Pollution Research Center, University of California, Riverside, California 92521-0001, United States

[§]Department of Atmospheric Science, Colorado State University, Fort Collins, Colorado 80523-1371, United States

Supporting Information

ABSTRACT: Organic aerosols in the atmosphere are composed of a wide variety of species, reflecting the multitude of sources and growth processes of these particles. Especially challenging is predicting how these particles act as cloud condensation nuclei (CCN). Previous studies have characterized the CCN efficiency for organic compounds in terms of a hygroscopicity parameter, κ. Here we extend these studies by systematically testing the influence of the number and location of molecular functional groups on the hygroscopicity of organic aerosols. Organic compounds synthesized via gas-phase and liquid-phase reactions were characterized by high-performance liquid chromatography coupled with scanning flow CCN analysis and thermal desorption particle beam mass spectrometry. These experiments quantified changes in κ with the addition of one or more functional groups to otherwise similar molecules. The increase in κ per group decreased in the following order: hydroxyl ≫ carboxyl > hydroperoxide > nitrate ≫ methylene (where nitrate and methylene produced negative effects, and hydroperoxide and nitrate groups produced the smallest absolute effects). Our results contribute to a mechanistic understanding of chemical aging and will help guide input and parametrization choices in models relying on simplified treatments such as the atomic oxygen:carbon ratio to predict the evolution of organic aerosol hygroscopicity.

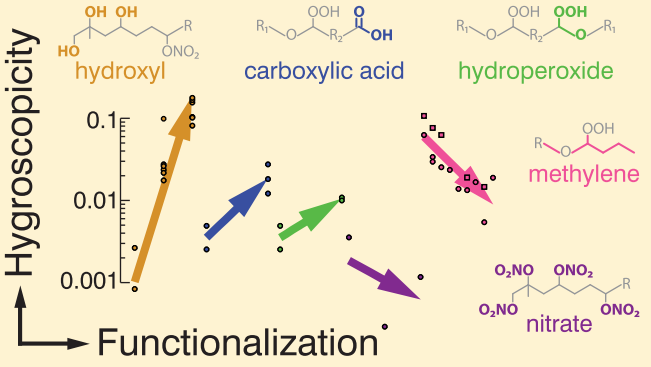

INTRODUCTION

Organic aerosols (OA) are an important contributor to submicrometer aerosol mass. The presence of OA in the atmosphere negatively impacts human well-being,[1,2] reduces visibility,[3,4] and alters the global radiative balance.[5] The atmospheric OA lifetime and the magnitude of the effect of OA on climate are closely tied to the particles' ability to serve as cloud condensation nuclei (CCN).[6−8] Freshly emitted OA generally consists of weakly oxidized and thus hydrophobic hydrocarbon chains.[9−11] In the atmosphere, these compounds age and evolve by functionalization, fragmentation, and oligomerization to form hydrophilic compounds on time scales from hours to days.[12,13] Current modeling approaches parametrize this conversion using empirical correlations between the atomic oxygen:carbon (O:C) ratio and observed hygroscopic growth factors[14] or CCN activity[15,16] expressed in terms of the hygroscopicity parameter, κ. This approach is attractive because it simplifies the complex links among hygroscopicity, solubility in water, surface tension, and molecular functional group composition.[17−19] However, a recent study by Rickards et al.[20] and a compiled body of experimental data summarized in Figure S1 of the Supporting Information show that the CCN activity for single-component organic aerosols cannot be explained by the current O:C approach. This discrepancy highlights the need for a more mechanistic understanding of the role OA oxidation plays in converting aerosol from CCN inactive to CCN active.

Here we present findings from a new approach to probing the influence of OA oxidation state on CCN activity. Our approach combines molecular synthesis of model compounds, similar to those present in the atmosphere but not commercially available, with high-performance liquid chromatography (HPLC) coupled to scanning flow CCN analysis.[21] By designing synthetic model compounds, we were able to extend studies[22] that vary only the type and location of a single

Received: May 1, 2014
Revised: July 24, 2014
Accepted: August 13, 2014
Published: August 13, 2014

Scheme 1. Mechanism for the Synthesis of Hydroperoxides[a]

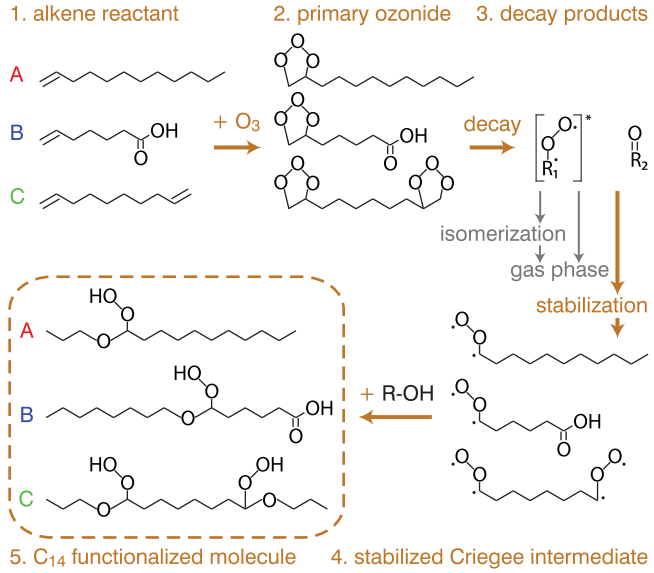

[a]Experiments A–C were performed as separate mixtures.

functional group, thus allowing the quantification of changes in κ with the addition of one or more functional groups to otherwise similar molecules. Experimental results reported in this paper demonstrate that the effect of adding hydroxyl groups to the carbon chain far exceeds that of carboxylic acid, hydroperoxide ether, and nitrate groups. This finding suggests that regardless of whether the oxidation mechanism is initiated by OH, O_3, or NO_3 it plays an important role in determining the hydrophobic-to-hydrophilic conversion time scale. This finding may further explain a multitude of observations demonstrating that organic compounds begin the conversion from hydrophobic to hydrophilic at surprisingly low O:C ratios ranging from 0.03 to ~0.2.[14−16,23−25]

MATERIALS AND METHODS

Five functional groups were targeted in this study: hydroxyl (−OH), hydroperoxide ether [−C(OOH)−O−], carboxylic acid [−C(=O)OH], nitrate ($-ONO_2$), and methylene ($-CH_2-$). These five functional groups were varied using hydroperoxides and hydroxynitrates as basic molecular building blocks. We first discuss the synthesis of these compounds followed by a description of the CCN analysis. Hydroperoxides with varying numbers of hydroperoxide ether and carboxylic acid groups were synthesized in the liquid phase using ozonolysis; hydroxynitrates with varying numbers of hydroxyl and nitrate groups and a second set of hydroperoxides with varying numbers of methylene groups were synthesized in environmental chambers as secondary organic aerosols (SOA) via gas-phase reactions. The structures of these and similar compounds are generally well established from the reaction mechanisms and have also been characterized in our previous studies using various combinations of HPLC (for separation and/or purification), thermal desorption particle beam mass spectrometry, electrospray ionization mass spectrometry, and nuclear magnetic resonance.[26−32] Procedures that were used to assign molecular structures to measured κ values are provided in the Supporting Information.

The first set of hydroperoxides was generated from the reaction of 1-alkenes,[27] alkenoic acids, and dienes with O_3 in the liquid phase. Liquid-phase synthesis was used because the products of interest are formed in high yields[26,27] and large amounts could easily be generated. Scheme 1 summarizes the three synthetic reaction mechanisms and the resulting model compounds. A full list of experiments is included in Table S1 of the Supporting Information. Ozone was bubbled through a 5:500:4500 (by volume) alkene/alcohol/acetonitrile liquid solution, with the moles of ozone added being approximately the same as the moles of alkene present. The ozone adds to the C=C bond of the alkene to form a primary ozonide (Scheme 1, 2) that rapidly decomposes by cleavage of the C−C bond and one of the O−O bonds to form a pair of functional groups: an aldehyde [−C(=O)H] and excited carbonyl oxide [−C(OO)H], which is also termed an excited Criegee intermediate (ECI) (Scheme 1, 3). For C_n 1-alkenes, four monofunctional products are formed, consisting of C_{n-1} and C_1 aldehydes and ECIs. For C_n 1,*n*-dienes, three C_{n-2} bifunctional products are formed: one with two aldehyde groups, one with two ECI groups, and one with an aldehyde and ECI group, all located at opposite ends of the molecule, in addition to C_1 aldehydes and ECIs. In all cases, the ECI groups undergo almost complete stabilization because of collisions with solvent molecules to form stabilized Criegee intermediates (SCIs) (Scheme 1, 4),[26] which then react with the large excess of alcohol to form α-alkoxyhydroperoxides (Scheme 1, 5). Volatile products such as aldehydes and reaction products of the C_1 SCI evaporated from the solution when it was atomized for aerosol formation as described below.

A second set of hydroperoxides was generated in an environmental chamber by ozonolysis of 1-alkenes in the gas phase (Scheme 1).[33] These experiments were performed in a 1.7 m^3 FEP Teflon film environmental chamber[34] that was operated at 25 °C and atmospheric pressure. Reactants were added in 0.3:10:700 ppmv 1-alkene/(methanol or propanol)/cyclohexane proportions and reacted with 0.7 ppmv O_3. The O_3:alkene ratio was sufficiently high to break all double bonds. Sampling was performed ~10 min after the addition of O_3, and measurements were completed after ~1 h. Cyclohexane scavenged OH radicals, which were not formed in liquid-

dx.doi.org/10.1021/es502147y | Environ. Sci. Technol. 2014, 48, 10182−10190

phase reactions described above, and air molecules stabilized a significant fraction of the ECIs. A trace amount of β-caryophyllene was added with reactants to produce seed aerosol by rapid ozonolysis and homogeneous nucleation of the reaction products.[21,35] This shifted the particle size distribution to facilitate the generation of a sufficient number of particles for analysis.[21,35] The expected average contribution of seed mass to total mass was <1%.[21] As with liquid-phase ozonolysis, SCI reacted solely with the excess alcohol to form α-alkoxyhydroperoxides (Scheme 1, 5A), which subsequently condensed to form SOA. The SOA formed by this method is comprised almost entirely of C_{n-1} α-alkoxyhydroperoxides, with a small fraction of C_{n-1} carboxylic acid formed by the isomerization of the C_{n-1} ECI.[21,27]

Hydroxynitrates were synthesized in the gas phase from the OH radical-initiated reaction of 2-methyl-1-alkenes in the presence of NO_x.[28,29] Scheme S1 of the Supporting Information shows the reaction mechanism. One ppmv of C_{10}−C_{15} 2-methyl-1-alkene precursor with 10 ppmv of both CH_3ONO and NO were introduced into a 7 m^3 PTFE Teflon environmental chamber[31] at room temperature and pressure and irradiated with a bank of UV blacklights ($\lambda_{max} \sim 360$ nm) for 6 min. Hydroxyl radicals were produced from photolysis of CH_3ONO in the presence of excess NO, which suppresses O_3 and NO_3 radical formation.[36] SOA formed from OH oxidation products was then collected on Teflon filters and extracted in ethyl acetate, and the ethyl acetate was then evaporated under vacuum. The major products are β-hydroxynitrates, dihydroxynitrates, trihydroxynitrates, and multifunctional hydroxycarbonyls.[28,29] Products are identified by HPLC retention time (discussed further in the Supporting Information). A fraction of the mixture was set aside for immediate CCN analysis, as described below. The other fraction was further reacted with N_2O_5 in a vacuum rack to convert hydroxyl groups to nitrate groups via the C−OH + N_2O_5 → C−ONO_2 + HNO_3 reaction.[30] The sample was extracted again, dried in a stream of N_2, and reconstituted with 1 mL of ethyl acetate/mg of sample.

Finally, complex SOA mixtures containing nitrate moieties were generated in the gas phase by reacting selected C_7−C_{14} linear, cyclic, and branched alkenes with NO_3 radicals formed from the thermal dissociation of N_2O_5. In these reactions, NO_3 radicals add to the C=C bond to form β-nitrooxyperoxy radicals that subsequently undergo self-reactions and reactions with NO_3 and NO_2 to form a complex mixture of multifunctional nitrates that contain hydroxyl and carbonyl groups in addition to the nitrate groups.[31] These experiments were conducted in a 1.7 m^3 environmental chamber;[34] materials used and synthesis of chemicals required to perform all of the reactions described above were identical to those reported previously.[28,29,31,33]

Two types of CCN analysis were performed. Liquid samples from the first set of hydroperoxide synthesis and filter extracts from chamber experiments were separated by HPLC and characterized by scanning flow CCN analysis.[21] SOA formed in the environmental chamber from the reactions of O_3 and NO_3 radicals with alkenes was sampled directly from the chamber for analysis using size-resolved CCN analysis.[37]

The HPLC−CCN setup was similar to that used previously.[21] The HPLC system employed reversed-phase gradient elution of acetonitrile and water with a Zorbax 5 μm Eclipse XDB-C18 column and a guard column. Atomized eluate passed through a charcoal denunder and silica gel dryer to remove solvents before being charge neutralized by a ^{210}Po neutralizer[38] (Aerosol Dynamics Inc., model 100). The aerosol was then size selected by a DMA (TSI 3071) and split between a CPC (TSI 3771) and a CCN counter (DMT) operated in scanning flow mode.[39] A constant D_d was selected for each supersaturation scan such that CCN activation was observed. Flow through the CCN counter was pulled by an external pump through a proportional valve. The flow scan cycle was reduced to 30 s (6 s hold, 24 s upscan) such that more than one activation curve was acquired during the 1−3 min elution of each chromatographic peak.

Figure 1 shows an example HPLC chromatogram excerpt. Each peak corresponds to two to three CCN activation spectra,

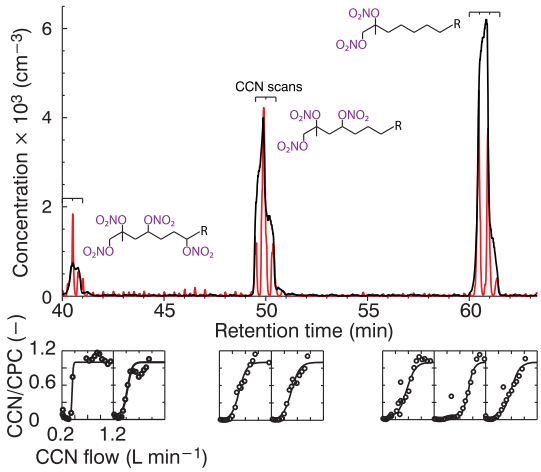

Figure 1. Chromatographic peaks from the C_{14} hydroxynitrate experiment. The top panel shows an abridged time series of total particles eluting from the HPLC setup counted by the CPC (black lines) and CCN active particles (red lines). The bottom row shows the resulting activation spectra for each flow scan with fitted sigmoidal activation curves.[21,55] The proposed compound structure is based on thermal desorption particle beam mass spectrometry.

which are plotted below the chromatogram. Samples from liquid synthesis or SOA extracts were divided to allow for multiple HPLC injections, and the reported κ values represent the average of three to four injections. Data pairs of s_c and D_d derived from individual scans and averaged κ values are listed in Tables S1 and S2 of the Supporting Information. The assignment of peaks to compounds is described further in the Supporting Information.

Size-resolved CCN activation spectra were measured with a setup similar to that of Petters et al.[37] The aerosol was size selected with a differential mobility analyzer (DMA; TSI 3071), and the flow was split between a condensation particle counter (CPC; TSI 3010) and a continuous flow CCN counter[40] (Droplet Measurements Technologies) held at a fixed water vapor supersaturation (s_c). Spectra were inverted to correct for multiple charges[37] to find the diameter at which 50% activation occurred. Although this method was slightly more accurate than the scanning flow method, it was slower, thus precluding its use in the HPLC−CCN analysis described above. A complete list of measurements performed in this manner is provided in Tables S3 and S4 of the Supporting Information.

Calibration of the CCN instrument supersaturation for all experiments was achieved with ammonium sulfate aerosol using the relationship between water activity and dilution from the Extended Aerosol Inorganics Model[41] (E-AIM). Calibration

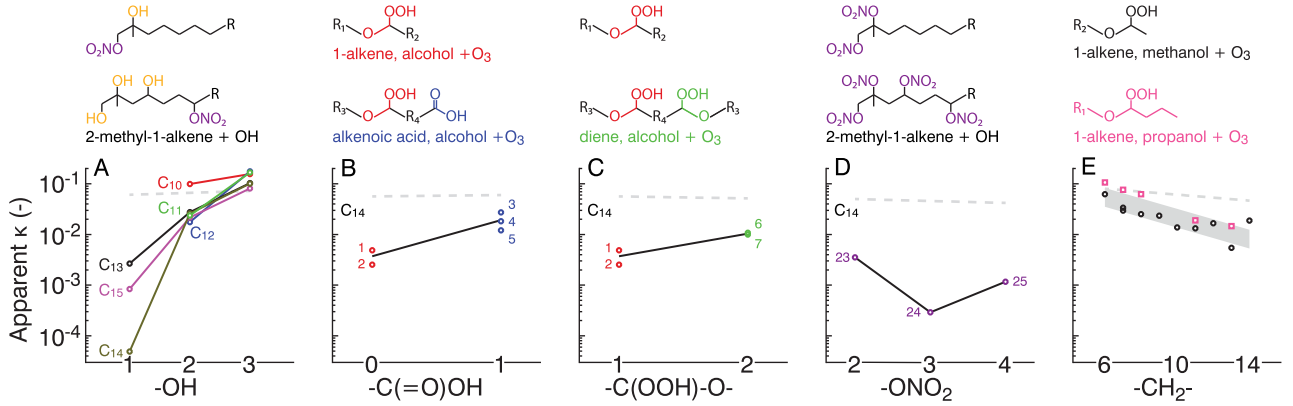

Figure 2. Results of experiments varying hydroxyl (A), carboxyl (B), hydroperoxide ether (C), nitrate (D), and methylene (E) groups. Scales are consistent across all panels, and the targeted molecular structures are summarized above the axes. Panels A and D show C_{10}−C_{15} hydroxynitrates and C_{14} nitrates from environmental chamber reactions; panels B and C show C_{14} hydroperoxides from liquid synthesis, and panel E shows C_9−C_{17} hydroperoxides from environmental chamber reactions with either methanol (black circles) or propanol (pink squares) as the Criegee scavenger. Dotted gray lines show estimated intrinsic κ values. All molecular synthesis procedures, product structures, and best-fit slopes are included in the Supporting Information. Numbers in panels B−D correspond to Tables S1 and S2 of the Supporting Information.

procedures of the diameter-dependent and scanning flow CCN techniques are further described by Christensen and Petters[42] and Suda et al.,[21] respectively. Supersaturation inferred from diameter scans typically fluctuates ±10%.[42] Flow scans from 0.2 to 1.2 L min^{-1} corresponded to levels of supersaturation from 0.17 to 1.16%, respectively. The uncertainty in supersaturation assignment during flow scans was evaluated from the calibration and is ±20%.

Paired D_d and s_c values were used to calculate the apparent hygroscopicity parameter, κ, at a standard state of T = 298 K and σ = 72 mJ m^{-2}.[17,42] Temperature (T) and surface tension (σ) are assumed to be constant, and the resulting "apparent κ" is used because it facilitates comparison between the relative ability of different compounds to promote CCN activity. The relative uncertainty in κ estimated from the supersaturation fluctuations is ±20 and ±40% for the size-resolved and flow-scan method, respectively. The minimal κ that can be resolved is determined by the maximal s (~1%) and D_d (~400 nm), corresponding to activation properties that are worse than those of insoluble but wettable particles described by κ = 0.

RESULTS AND DISCUSSION

Figure 2 shows the changes in CCN efficiency for molecules as a function of type and location of functional groups, arranged by decreasing d $\log_{10}(\kappa)/dn_i$ where n is the number of functional groups of type i. Values for κ and slopes d $\log_{10}(\kappa)$/dn and d $\log_{10}(\kappa)$/d(O:C) are listed in Table S5 of the Supporting Information. A change of more than 2 orders of magnitude in κ was observed for the addition of two hydroxyl groups to C_{10}−C_{15} hydroxynitrates (panel A). We note that C_{10}−C_{12} β-hydroxynitrates were too volatile for measurement, although the corresponding di- and trihydroxynitrates were captured. The effectiveness of hydroxyl groups in facilitating hydration is also well-known from the adsorption of water on metals[43] or metal oxides.[44−47] Results for C_{14} hydroperoxides with and without a terminal carboxyl group (panel B) show that the carboxyl group tends to increase a molecule's κ and that this trend systematically varies with the location of the hydroperoxide group. For hydroperoxides formed from 1-alkenes and alkenoic acids (panel B), compounds with the hydroperoxide group closer to the center of the molecule (indicated by the numbers 1−5 corresponding to structures in Table S1 of the Supporting Information) have κ values slightly higher than those of compounds with the hydroperoxide group closer to the end of the molecule. This observation is consistent with the theory that polar functional groups increase a molecule's affinity for water more effectively when they are located closer to the molecule's center.[48] The difference between these isomers is relatively small and close to the uncertainty limit that our method can resolve reliably. Such small differences are unlikely to result in significant differences in the CCN activity of a complex OA mixture in the atmosphere. Adding a second hydroperoxide group also increased κ (panel C), although to a lesser extent than carboxyl groups.

Increasing the number of nitrate groups (panel D) led to a slight decrease in κ, which is expected because of the low solubility of organic nitrates[49] and consistent with the results of environmental chamber experiments in which additional nitrates were generated (Table S4 of the Supporting Information). With the exception of the cyclooctene reaction, SOA formed in this manner proved to be CCN inactive for particles having a D_d of <400 nm and an s_c of 0.78%.

Hydroperoxides formed with a range of carbon numbers from chamber reactions (panel E) exhibited a decrease in κ by 1 order of magnitude upon addition of eight methylene (−CH_2−) groups. For reactions in which methanol is used as the SCI scavenger, the hydroperoxide group is closer to the end of the carbon chain than when propanol is used. Upon comparison of molecules with identical carbon chain lengths, those with hydroperoxide groups closer to the center of the molecule show systematically larger κ values. This effect agrees with and is similar in magnitude to the results for hydroperoxides with a terminal carboxyl group (panel B).

Figure 3 shows κ for molecules as a function of their O:C ratios. These ratios were calculated from the molecular structures. For molecules with different numbers of hydroxyl or methylene groups, there is a strong trend of increasing κ with increasing O:C ratio, consistent with previous observations.[14,15] We point out that there is likely an upper limit of κ ~ 0.3 beyond which OA κ cannot increase,[43] suggesting that empirical O:C ratio versus κ relationships need to be capped. Furthermore, the other systems (corresponding to Figure 2B−D) show no increase or only a slight increase in κ with O:C ratio. Most of these compounds have κ values of less than

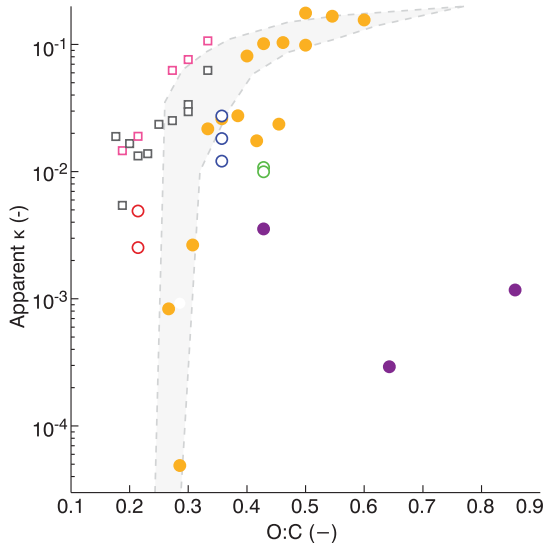

Figure 3. Plot of κ vs O:C ratio. Colors indicate the functional group targeted: gold for hydroxyl (−OH) (Figure 2A), blue for carboxylic acid [−C(=O)OH] (Figure 2B), green for hydroperoxide ether [−C(OOH)−O−] (Figure 2C), purple for nitrate ($-ONO_2$) (Figure 2D), and black and pink for methylene ($-CH_2-$) (Figure 2E). Empty symbols correspond to hydroperoxides (circle, liquid synthesis; square, chamber reaction). Filled symbols correspond to hydroxynitrates. The shaded region traces the data reported by Jimenez et al.[14]

~0.02, and we consider those effectively CCN inactive. Many of the empirical O:C ratio versus κ relationships in the literature are built from aerosol mass spectrometer data. Those measurements typically do not include nitrate groups in the estimates of O:C ratios because of analytical difficulties[50] and thus underestimate the O:C ratio of the organic fraction of aerosol. To compare our data to aerosol mass spectrometer data, we simulated this artifact by recalculating the O:C ratio for nitrate-containing compounds assuming only one O per ONO_2 group (similar to loss of NO_2 in an aerosol mass spectrometer). The scatter between O:C ratio and κ is reduced when our data are recast in this manner (Figure S2 of the Supporting Information), although significant spread remains. Furthermore, the transition from low κ to high κ begins at an O:C ratio of <0.2.

At the process level, κ is intrinsically determined by the size of the organic molecule, i.e., its molecular volume,[51] but this "intrinsic κ" (also known as κ_{ideal} or the Raoult term in an ideal Köhler curve)[52,53] can be suppressed if the compound is not sufficiently soluble in water.[18,54] Sufficiently soluble compounds are those that activate in accordance with intrinsic κ with small deviations due to solution nonideality[54] and surface tension depression.[19] Insoluble and sparingly soluble compounds must undergo a solubility-controlled phase transition prior to CCN activation. For sparingly soluble compounds, the resulting κ is strongly dependent on the actual solubility,[18,42,55] typically falling into the range of 0.01−0.001.[54] Given these controls on κ, the conversion from low to high κ due to the addition of functional groups corresponds to the conversion of a molecule from insoluble to sufficiently soluble in water.[25,56] Compounds close to that transition will require only one or two additional functional groups to dramatically age from a solubility-limited κ to an intrinsic κ determined by molecular volume, which typically exceeds 0.1 for molecules that have fewer than 15 carbon atoms. Figure 2 shows that measured κ values approach the intrinsic κ estimated from molecular volume,[69] which is consistent with such a transition. Note that for sparingly soluble compounds the dry particle diameter also influences the apparent κ because of its effect on deliquescence.[18] In this study, the particle diameter was dictated by experimental constraints and not varied systematically. Some of the observed trends could be masked or magnified if different sizes were used. Despite this limitation, the results clearly demonstrate that the degree of functionalization required to bring a molecule close to this solubility transition range depends on the carbon chain length and type of functional group.

Evidence from prior OA aging studies[14−16,23−25] clearly demonstrates that the low- to high-κ transition starts at mass spectrometer-derived O:C ratios of <0.2 and is complete at an O:C ratio of ~0.5. However, pure adipic acid [HOOC−$(CH_2)_4$−COOH, O:C ratio of 0.66] and larger dicarboxylic acids are not sufficiently soluble and thus cannot express their intrinsic κ.[42,56−58] For example, the observed apparent κ for adipic acid is between 0.001 and 0.01.[42] Counterexamples such as adipic acid highlight the need for a mechanistic explanation for the empirically derived close association between the O:C ratio and κ. The relative tightness of the observed empirical O:C ratio versus κ relation from field studies superimposed in Figure 3 is surprising because the O:C ratio is independent of carbon chain length and moieties associated with the carbon backbone: a hypothetical C_{20} dihydroperoxide ether [C_{16}(C−O−C−OOH)$_2$], a C_{10} trihydroxide [$C_{10}H_x(OH)_3$], and a C_{10} nitrate ($C_{10}H_xONO_2$) have identical O:C ratios of 0.3 but differ widely in molecular volume and water solubility. Can our results explain the discrepancy between the understanding of the process and the empirical observations?

The main result of this study is that hydroxyl functional groups and the length of the hydrophobic aliphatic chains are the dominant drivers of the solubility transition. The addition of hydroxyl groups thus helps remove solubility limitations and significantly increases the apparent κ value. Oxygen atoms associated with carboxylic acids, hydroperoxides, and nitrates do not contribute strongly to changes in κ because of the known ineffectiveness of nitrate[49] and carboxyl groups[70] to promote particle solubility. We point out that the compounds used to test the influence of the hydroxyl group on κ (Figure 2A) are multifunctional. Thus, the result may have been modulated by nitrate−hydroxyl group interactions and/or the combined effects of the hydroxyl and nitrate groups on promoting solubility. Preliminary results modeling the solubility transition using the semiempirical UNIFAC approach[59] suggest that the most important group interaction terms are those of functional group i with water; interactions of groups i and j appear to be minor. However, fully untangling group additivity and group−group interaction effects on CCN activity will require concerted efforts between thermodynamic modeling and experiments validating model predictions. Interpretation of these findings is further complicated by the presence of inorganic compounds in atmospheric particles. For insoluble organics internally mixed with soluble inorganics, the resultant κ is likely well described by the volume-weighted average κ of the components.[17] Compounds close to the solubility transition that are classified as sparingly soluble may undergo codissolution supported by the water associated with the inorganic compound in solution and thus may express higher organic κ values in mixed particles as compared to measurements of the pure compound.[18,60]

These results may explain the apparent discrepancies in studies that simulate the hydrophobic-to-hydrophilic transition during heterogeneous chemical aging of primary organic aerosols. Petters et al.[61] did not observe an increase in κ for linoleic acid ($C_{18}H_{32}O_2$) after the additioon of functional groups to the carbon backbone via reaction of NO_3 radicals with the C=C bond. The final product consisted of a nitrate:carbonyl:hydroxyl ratio of ~2:1:1 and increased the O:C ratio from 0.11 to >0.4. Later heterogeneous aging studies via OH radical oxidation[25,62] showed much more rapid conversion of squalane ($C_{30}H_{62}$), bis(2-ethylhexyl) sebacate [$(CH_2)_8(COOC_8H_{17})_2$], and stearic acid ($C_{18}H_{36}O_2$) starting at O:C ratios as low as 0.03. Heterogeneous oxidation with OH radicals starts with abstraction of a H atom from the carbon chain leading to the addition of primarily hydroxyl and carbonyl groups with minor contributions of hydroperoxy groups.[63] The stark difference between the linoleic acid and squalane aging models can likely be explained by the known ineffectiveness of nitrate and carboxyl groups to promote particle solubility. Conversely, the hydroxyl groups generated by OH radical-initiated aging, combined with the fact that OH radical-initiated aging leads to a statistical distribution of oxidation products within the particle containing a small fraction of more highly functionalized molecules,[63] can explain the effectiveness of OH radical attack in increasing κ.

Heald et al.[64] found that OA composition from a variety of environments occupies a narrow range following a slope of approximately −1 when graphing elemental composition in the H:C versus O:C state space (Van Krevelen diagram). This suggests that functionalization proceeds in a manner consistent with increases in either hydroxyl/carbonyl pairs or in carboxylic acid groups. Combining the aging results that show rapid hydrophobic-to-hydrophilic conversion at low O:C ratios with the fact that organic acids are terminal moieties and relatively poor in promoting solubility,[70] we suggest that hydroxylation may be an important pathway by which aerosols become more hygroscopic. Some observations support the dominance of hydroxyl groups over carboxyl groups in ambient OA. For example, the ratio of hydroxyl to carboxyl groups in SOA formed from monoterpene oxidation in a forest is ~2.7:1.[65] Tight empirical correlations between the O:C ratio and κ in field[14,15] and laboratory studies[16,23] combined with the dominant compositional trajectory in different environments following a slope of −1 in Van Krevelen space may reflect a ubiquitous and relatively unchanging mechanism of evolving aerosol composition and hygroscopicity. Our interpretation of the empirical O:C ratio versus κ observation is that it provides a constraint on predominant chemical aging mechanisms in the atmosphere more than a reliable predictor of CCN activity.

The significance of the OH group in OA transformations emphasizes the importance of chemical mechanisms that lead to the addition of hydroxyl groups. In the gas phase, hydroxyl groups are added by the addition of OH radicals to the C=C bond and isomerization of the alkoxy radical.[13] In the condensed phase, the self-reactions of RO_2 radicals[13] or hydrolysis of organic nitrates[66,67] contributes to the addition of OH groups. On the basis of these findings, we make the following testable predictions.

(1) Ambient OA κ will correlate with the hydroxyl group fraction under conditions where solubility limits the ability of OA to express its intrinsic κ.

(2) OA formation and heterogeneous chemistry that proceeds in unique settings, such as nighttime oxidation by NO_3 radicals or laboratory aging experiments that do not follow the Van Krevelen slope of −1 (e.g., heterogeneous oxidation of squalane),[64,68] will result in divergent relationships between the O:C ratio and κ.

(3) Heterogeneous chemistry that leads to condensed-phase transformation of functional groups, such as hydrolysis of organic nitrates to alcohols,[66,67] will result in accelerated aging of OA in the atmosphere.

Future studies are needed to test these hypotheses.

■ ASSOCIATED CONTENT

Supporting Information

Additional methods, figures, tables, and references. This material is available free of charge via the Internet at http://pubs.acs.org.

■ AUTHOR INFORMATION

Corresponding Author

*Department of Marine Earth and Atmospheric Sciences, North Carolina State University, Campus Box 8208, Raleigh, NC 27695. E-mail: markus_petters@ncsu.edu.

Present Addresses

[¶]G.K.Y.: Pearl Therapeutics, 200 Saginaw Drive, Redwood City, CA 94063-4725.

[‖]C.S.: Department of Chemistry, College of St. Benedict and St. John's University, St. Joseph, MN 56374.

[⊥]A.M.: California Air Resources Board, Emissions Compliance, Automotive Regulations and Sciences Division, El Monte, CA 91731.

[@]P.J.Z.: Department of Chemistry and Biochemistry, University of Colorado, Boulder, CO 80302.

[▽]A.J.P.: Air Resources Division, National Park Service, Lakewood, CO 80228.

[#]C.M.C.: Department of Civil and Environmental Engineering, New Mexico Institute of Mining and Technology, Socorro, NM 87801.

[●]R.C.S.: Center for Atmospheric Particle Studies, Carnegie Mellon University, Pittsburgh, PA 15213.

Author Contributions

All authors contributed to conducting the measurements and interpreting the data. M.D.P., P.J.Z., and S.M.K. designed the study. S.R.S. and M.D.P. wrote the manuscript. All authors have given approval to the final version of the manuscript.

Funding

This research was funded by the Department of Energy, Office of Biological and Environmental Sciences, via Grant DE-SC0006633.

Notes

The authors declare no competing financial interest.

■ ACKNOWLEDGMENTS

We thank April Ranney for her help with synthesizing some of the compounds. We thank Mary Gilles for discussion of the results.

■ REFERENCES

(1) Dockery, D. W.; Pope, C. A.; Xu, X.; Spengler, J. D.; Ware, J. H.; Fay, M. E.; Ferris, B. G.; Speizer, F. E. An association between air pollution and mortality in six U.S. cities. *N. Engl. J. Med.* **1993**, *329* (24), 1753−1759.

(2) Gaschen, A.; Lang, D.; Kalberer, M.; Savi, M.; Geiser, T.; Gazdhar, A.; Lehr, C.; Bur, M.; Dommen, J.; Baltensperger, U.; Geiser,

M. Cellular responses after exposure of lung cell cultures to secondary organic aerosol particles. *Environ. Sci. Technol.* **2010**, *44* (4), 1424−1430.
(3) Groblicki, P. J.; Wolff, G. T.; Countess, R. J. Visibility-reducing species in the Denver "brown cloud" I. Relationships between extinction and chemical composition. *Atmos. Environ.* **1981**, *15* (12), 2473−2484.
(4) Malm, W. C.; Sisler, J. F.; Huffman, D.; Eldred, R. A.; Cahill, T. A. Spatial and seasonal trends in particle concentration and optical extinction in the United States. *J. Geophys. Res.* **1994**, *99*, 1347−1370.
(5) Twomey, S. A. Pollution and the planetary albedo. *Atmos. Environ.* **1974**, *8* (12), 1251−1256.
(6) Heintzenberg, J. Fine particles in the global troposphere A review. *Tellus, Ser. B* **1989**, *41* (2), 149−160.
(7) Raes, F.; Dingenen, R. V.; Vignati, E.; Wilson, J.; Putaud, J.; Seinfeld, J. H.; Adams, P. Formation and cycling of aerosols in the global troposphere. *Atmos. Environ.* **2000**, *34* (25), 4215−4240.
(8) Kanakidou, M.; Seinfeld, J. H.; Pandis, S. N.; Barnes, I.; Dentener, F. J.; Facchini, M. C.; Van Dingenen, R.; Ervens, B.; Nenes, A.; Nielsen, C. J.; Swietlicki, E.; Putaud, J.; Balkanski, Y.; Fuzzi, S.; Horth, J.; Moortgat, G. K.; Winterhalter, R.; Myhre, C. E. L.; Tsigaridis, K.; Vignati, E.; Stephanou, E. G.; Wilson, J. Organic aerosol and global climate modelling: A review. *Atmos. Chem. Phys.* **2005**, *5* (4), 1053−1123.
(9) Broekhuizen, K. E.; Thornberry, T.; Kumar, P. P.; Abbatt, J. P. D. Formation of cloud condensation nuclei by oxidative processing: Unsaturated fatty acids. *J. Geophys. Res.* **2004**, *109*, D24206.
(10) Zhang, Q.; Jimenez, J. L.; Canagaratna, M. R.; Allan, J. D.; Coe, H.; Ulbrich, I.; Alfarra, M. R.; Takami, A.; Middlebrook, A. M.; Sun, Y. L.; Dzepina, K.; Dunlea, E. J.; Docherty, K. S.; DeCarlo, P. F.; Salcedo, D.; Onasch, T.; Jayne, J. T.; Miyoshi, T.; Shimono, A.; Hatakeyama, S.; Takegawa, N.; Kondo, Y.; Schneider, J.; Drewnick, F.; Borrmann, S.; Weimer, S.; Demerjian, K.; Williams, P.; Bower, K.; Bahreini, R.; Cottrell, L.; Griffin, R. J.; Rautiainen, J.; Sun, J. Y.; Zhang, Y. M.; Worsnop, D. R. Ubiquity and dominance of oxygenated species in organic aerosols in anthropogenically-influenced Northern Hemisphere midlatitudes. *Geophys. Res. Lett.* **2007**, *34* (13), L13801.
(11) Aiken, A. C.; DeCarlo, P. F.; Kroll, J. H.; Worsnop, D. R.; Huffman, J. A.; Docherty, K. S.; Ulbrich, I. M.; Mohr, C.; Kimmel, J. R.; Sueper, D.; Sun, Y.; Zhang, Q.; Trimborn, A.; Northway, M.; Ziemann, P. J.; Canagaratna, M. R.; Onasch, T. B.; Alfarra, M. R.; Prévôt, A. S. H.; Dommen, J.; Duplissy, J.; Metzger, A.; Baltensperger, U.; Jimenez, J. L. O/C and OM/OC ratios of primary, secondary, and ambient organic aerosols with high-resolution time-of-flight aerosol mass spectrometry. *Environ. Sci. Technol.* **2008**, *42* (12), 4478−4485.
(12) Kroll, J. H.; Seinfeld, J. H. Chemistry of secondary organic aerosol: Formation and evolution of low-volatility organics in the atmosphere. *Atmos. Environ.* **2008**, *42* (16), 3593−3624.
(13) Ziemann, P. J.; Atkinson, R. Kinetics, products, and mechanisms of secondary organic aerosol formation. *Chem. Soc. Rev.* **2012**, *41* (19), 6582−6605.
(14) Jimenez, J. L.; Canagaratna, M. R.; Donahue, N. M.; Prévôt, A. S. H.; Zhang, Q.; Kroll, J. H.; DeCarlo, P. F.; Allan, J. D.; Coe, H.; Ng, N. L.; Aiken, A. C.; Docherty, K. S.; Ulbrich, I. M.; Grieshop, A. P.; Robinson, A. L.; Duplissy, J.; Smith, J. D.; Wilson, K. R.; Lanz, V. A.; Hueglin, C.; Sun, Y. L.; Tian, J.; Laaksonen, A.; Raatikainen, T.; Rautiainen, J.; Vaattovaara, P.; Ehn, M.; Kulmala, M.; Tomlinson, J. M.; Collins, D. R.; Cubison, M. J.; Dunlea, E. J.; Huffman, J. A.; Onasch, T. B.; Alfarra, M. R.; Williams, P. I.; Bower, K.; Kondo, Y.; Schneider, J.; Drewnick, F.; Borrmann, S.; Weimer, S.; Demerjian, K.; Salcedo, D.; Cottrell, L.; Griffin, R.; Takami, A.; Miyoshi, T.; Hatakeyama, S.; Shimono, A.; Sun, J. Y.; Zhang, Y. M.; Dzepina, K.; Kimmel, J. R.; Sueper, D.; Jayne, J. T.; Herndon, S. C.; Trimborn, A. M.; Williams, L. R.; Wood, E. C.; Middlebrook, A. M.; Kolb, C. E.; Baltensperger, U.; Worsnop, D. R. Evolution of organic aerosols in the atmosphere. *Science* **2009**, *326* (5959), 1525−1529.
(15) Chang, R. Y.-W.; Slowik, J. G.; Shantz, N. C.; Vlasenko, A.; Liggio, J.; Sjostedt, S. J.; Leaitch, W. R.; Abbatt, J. P. D. The hygroscopicity parameter (κ) of ambient organic aerosol at a field site subject to biogenic and anthropogenic influences: Relationship to degree of aerosol oxidation. *Atmos. Chem. Phys.* **2010**, *10* (11), 5047−5064.
(16) Lambe, A. T.; Onasch, T. B.; Massoli, P.; Croasdale, D. R.; Wright, J. P.; Ahern, A. T.; Williams, L. R.; Worsnop, D. R.; Brune, W. H.; Davidovits, P. Laboratory studies of the chemical composition and cloud condensation nuclei (CCN) activity of secondary organic aerosol (SOA) and oxidized primary organic aerosol (OPOA). *Atmos. Chem. Phys.* **2011**, *11* (17), 8913−8928.
(17) Petters, M. D.; Kreidenweis, S. M. A single parameter representation of hygroscopic growth and cloud condensation nucleus activity. *Atmos. Chem. Phys.* **2007**, *7* (8), 1961−1971.
(18) Petters, M. D.; Kreidenweis, S. M. A single parameter representation of hygroscopic growth and cloud condensation nucleus activity. Part 2: Including solubility. *Atmos. Chem. Phys.* **2008**, *8* (20), 6273−6279.
(19) Petters, M. D.; Kreidenweis, S. M. A single parameter representation of hygroscopic growth and cloud condensation nucleus activity. Part 3: Including surfactant partitioning. *Atmos. Chem. Phys.* **2013**, *13* (2), 1081−1091.
(20) Rickards, A. M. J.; Miles, R. E. H.; Davies, J. F.; Marshall, F. H.; Reid, J. P. Measurements of the sensitivity of aerosol hygroscopicity and the κ parameter to the O/C ratio. *J. Phys. Chem. A* **2013**, *117* (51), 14120−14131.
(21) Suda, S. R.; Petters, M. D.; Matsunaga, A.; Sullivan, R. C.; Ziemann, P. J.; Kreidenweis, S. M. Hygroscopicity frequency distributions of secondary organic aerosols. *J. Geophys. Res.* **2012**, *117*, D04207.
(22) Frosch, M.; Zardini, A. A.; Platt, S. M.; Müller, L.; Reinnig, M.-C.; Hoffmann, T.; Bilde, M. Thermodynamic properties and cloud droplet activation of a series of oxo-acids. *Atmos. Chem. Phys.* **2010**, *10* (13), 5873−5890.
(23) Massoli, P.; Lambe, A. T.; Ahern, A. T.; Williams, L. R.; Ehn, M.; Mikkilä, J.; Canagaratna, M. R.; Brune, W. H.; Onasch, T. B.; Jayne, J. T.; Petäjä, T.; Kulmala, M.; Laaksonen, A.; Kolb, C. E.; Davidovits, P.; Worsnop, D. R. Relationship between aerosol oxidation level and hygroscopic properties of laboratory generated secondary organic aerosol (SOA) particles. *Geophys. Res. Lett.* **2010**, *37* (24), L24801.
(24) Cappa, C. D.; Che, D. L.; Kessler, S. H.; Kroll, J. H.; Wilson, K. R. Variations in organic aerosol optical and hygroscopic properties upon heterogeneous OH oxidation. *J. Geophys. Res.* **2011**, *116*, D15204.
(25) Harmon, C. W.; Ruehl, C. R.; Cappa, C. D.; Wilson, K. R. A statistical description of the evolution of cloud condensation nuclei activity during the heterogeneous oxidation of squalane and bis(2-ethylhexyl) sebacate aerosol by hydroxyl radicals. *Phys. Chem. Chem. Phys.* **2013**, *15* (24), 9679−9693.
(26) Bailey, P. S. The reactions of ozone with organic compounds. *Chem. Rev.* **1958**, *58* (5), 925−1010.
(27) Tobias, H. J.; Ziemann, P. J. Thermal desorption mass spectrometric analysis of organic aerosol formed from reactions of 1-tetradecene and O_3 in the presence of alcohols and carboxylic acids. *Environ. Sci. Technol.* **2000**, *34* (11), 2105−2115.
(28) Matsunaga, A.; Ziemann, P. J. Yields of β-hydroxynitrates and dihydroxynitrates in aerosol formed from OH radical-initiated reactions of linear alkenes in the presence of NO_x. *J. Phys. Chem. A* **2009**, *113* (3), 599−606.
(29) Matsunaga, A.; Ziemann, P. J. Yields of β-hydroxynitrates, dihydroxynitrates, and trihydroxynitrates formed from OH radical-initiated reactions of 2-methyl-1-alkenes. *Proc. Natl. Acad. Sci. U.S.A.* **2010**, *107* (15), 6664−6669.
(30) Kames, J.; Schurath, U.; Flocke, F.; Volz-Thomas, A. Preparation of organic nitrates from alcohols and N_2O_5 for species identification in atmospheric samples. *J. Atmos. Chem.* **1993**, *16* (4), 349−359.
(31) Gong, H.; Matsunaga, A.; Ziemann, P. J. Products and mechanism of secondary organic aerosol formation from reactions of

linear alkenes with NO_3 radicals. *J. Phys. Chem. A* **2005**, *109* (19), 4312−4324.
(32) Ziemann, P. J. Aerosol products, mechanisms, and kinetics of heterogeneous reactions of ozone with oleic acid in pure and mixed particles. *Faraday Discuss.* **2005**, *130*, 469−490.
(33) Tobias, H. J.; Ziemann, P. J. Kinetics of the gas-phase reactions of alcohols, aldehydes, carboxylic acids, and water with the C13 stabilized Criegee intermediate formed from ozonolysis of 1-tetradecene. *J. Phys. Chem. A* **2001**, *105* (25), 6129−6135.
(34) Matsunaga, A.; Ziemann, P. J. Gas-wall partitioning of organic compounds in a Teflon film chamber and potential effects on reaction product and aerosol yield measurements. *Aerosol Sci. Technol.* **2010**, *44* (10), 881−892.
(35) Prenni, A. J.; Petters, M. D.; Faulhaber, A.; Carrico, C. M.; Ziemann, P. J.; Kreidenweis, S. M.; DeMott, P. J. Heterogeneous ice nucleation measurements of secondary organic aerosol generated from ozonolysis of alkenes. *Geophys. Res. Lett.* **2009**, *36* (6), L06808.
(36) Atkinson, R.; Carter, W. P. L.; Winer, A. M.; Pitts, J. N. An experimental protocol for the determination of OH radical rate constants with organics using methyl nitrite photolysis as an OH radical source. *J. Air Pollut. Control Assoc.* **1981**, *31*, 1090−1092.
(37) Petters, M. D.; Carrico, C. M.; Kreidenweis, S. M.; Prenni, A. J.; DeMott, P. J.; Collett, J. L., Jr.; Moosmüller, H. Cloud condensation nucleation activity of biomass burning aerosol. *J. Geophys. Res.* **2009**, *114*, D22205.
(38) Russell, L. M.; Zhang, S.; Flagan, R. C.; Seinfeld, J. H.; Stolzenburg, M. R.; Caldow, R. Radially classified aerosol detector for aircraft-based submicron aerosol measurements. *Journal of Atmospheric and Oceanic Technology* **1996**, *13* (3), 598−609.
(39) Moore, R. H.; Nenes, A. Scanning flow CCN analysis: A method for fast measurements of CCN spectra. *Aerosol Sci. Technol.* **2009**, *43* (12), 1192−1207.
(40) Roberts, G. C.; Nenes, A. A continuous-flow streamwise thermal-gradient CCN chamber for atmospheric measurements. *Aerosol Sci. Technol.* **2005**, *39* (3), 206−221.
(41) Clegg, S. L.; Brimblecombe, P.; Wexler, A. S. Thermodynamic model of the system H^+−NH_4^+−Na^+−SO_4^{2-}−NO_3^-−Cl^-−H_2O at 298.15 K. *J. Phys. Chem. A* **1998**, *102* (12), 2155−2171.
(42) Christensen, S. I.; Petters, M. D. The role of temperature in cloud droplet activation. *J. Phys. Chem. A* **2012**, *116* (39), 9706−9717.
(43) Yamamoto, S.; Andersson, K.; Bluhm, H.; Ketteler, G.; Starr, D. E.; Schiros, T.; Ogasawara, H.; Pettersson, L. G. M.; Salmeron, M.; Nilsson, A. Hydroxyl-induced wetting of metals by water at near-ambient conditions. *J. Phys. Chem. C* **2007**, *111* (22), 7848−7850.
(44) Ketteler, G.; Yamamoto, S.; Bluhm, H.; Andersson, K.; Starr, D. E.; Ogletree, D. F.; Ogasawara, H.; Nilsson, A.; Salmeron, M. The nature of water nucleation sites on TiO_2(110) surfaces revealed by ambient pressure X-ray photoelectron spectroscopy. *J. Phys. Chem. C* **2007**, *111* (23), 8278−8282.
(45) Yamamoto, S.; Kendelewicz, T.; Newberg, J. T.; Ketteler, G.; Starr, D. E.; Mysak, E. R.; Andersson, K. J.; Ogasawara, H.; Bluhm, H.; Salmeron, M.; Brown, G. E.; Nilsson, A. Water adsorption on α-Fe_2O_3(0001) at near ambient conditions. *J. Phys. Chem. C* **2010**, *114* (5), 2256−2266.
(46) Newberg, J. T.; Starr, D. E.; Yamamoto, S.; Kaya, S.; Kendelewicz, T.; Mysak, E. R.; Porsgaard, S.; Salmeron, M. B.; Brown, G. E.; Nilsson, A.; Bluhm, H. Autocatalytic surface hydroxylation of MgO(100) terrace sites observed under ambient conditions. *J. Phys. Chem. C* **2011**, *115* (26), 12864−12872.
(47) Kendelewicz, T.; Kaya, S.; Newberg, J. T.; Bluhm, H.; Mulakaluri, N.; Moritz, W.; Scheffler, M.; Nilsson, A.; Pentcheva, R.; Brown, G. E. X-ray photoemission and density functional theory study of the interaction of water vapor with the Fe_3O_4(001) surface at near-ambient conditions. *J. Phys. Chem. C* **2013**, *117* (6), 2719−2733.
(48) Schwarzenbach, R. P.; Gschwend, P. M.; Imboden, D. M. *Environmental organic chemistry*, 1st ed.; John Wiley & Sons: New York, 1993.
(49) Boschan, R.; Merrow, R. T.; van Dolah, R. W. The chemistry of nitrate esters. *Chem. Rev.* **1955**, *55* (3), 485−510.
(50) Farmer, D. K.; Matsunaga, A.; Docherty, K. S.; Surratt, J. D.; Seinfeld, J. H.; Ziemann, P. J.; Jimenez, J. L. Response of an aerosol mass spectrometer to organonitrates and organosulfates and implications for atmospheric chemistry. *Proc. Natl. Acad. Sci. U.S.A.* **2010**, *107* (15), 6670−6675.
(51) Petters, M. D.; Kreidenweis, S. M.; Prenni, A. J.; Sullivan, R. C.; Carrico, C. M.; Koehler, K. A.; Ziemann, P. J. Role of molecular size in cloud droplet activation. *Geophys. Res. Lett.* **2009**, *36* (22), L22801.
(52) Suda, S. R.; Petters, M. D. Accurate determination of aerosol activity coefficients at relative humidities up to 99% using the hygroscopicity tandem differential mobility analyzer technique. *Aerosol Sci. Technol.* **2013**, *47* (9), 991−1000.
(53) Seinfeld, J. H.; Pandis, S. N. *Atmospheric chemistry and physics: From air pollution to climate change*; John Wiley & Sons: Hoboken, NJ, 2006; pp 1203.
(54) Petters, M. D.; Wex, H.; Carrico, C. M.; Hallbauer, E.; Massling, A.; McMeeking, G. R.; Poulain, L.; Wu, Z.; Kreidenweis, S. M.; Stratmann, F. Towards closing the gap between hygroscopic growth and activation for secondary organic aerosol. Part 2: Theoretical approaches. *Atmos. Chem. Phys.* **2009**, *9* (12), 3999−4009.
(55) Sullivan, R. C.; Moore, M. J. K.; Petters, M. D.; Kreidenweis, S. M.; Roberts, G. C.; Prather, K. A. Effect of chemical mixing state on the hygroscopicity and cloud nucleation properties of calcium mineral dust particles. *Atmos. Chem. Phys.* **2009**, *9* (10), 3303−3316.
(56) Kuwata, M.; Shao, W.; Lebouteiller, R.; Martin, S. T. Classifying organic materials by oxygen-to-carbon elemental ratio to predict the activation regime of cloud condensation nuclei (CCN). *Atmos. Chem. Phys.* **2013**, *13* (10), 5309−5324.
(57) Hori, M.; Ohta, S.; Murao, N.; Yamagata, S. Activation capability of water soluble organic substances as CCN. *J. Aerosol Sci.* **2003**, *34* (4), 419−448.
(58) Bilde, M.; Svenningsson, B. CCN activation of slightly soluble organics: The importance of small amounts of inorganic salt and particle phase. *Tellus, Ser. B* **2004**, *56* (2), 128−134.
(59) Fredenslund, A.; Jones, R. L.; Prausnitz, J. M. Group-contribution estimation of activity coefficients in nonideal liquid mixtures. *AIChE J.* **1975**, *21* (6), 1086−1099.
(60) Shulman, M. L.; Jacobson, M. C.; Carlson, R. J.; Synovec, R. E.; Young, T. E. Dissolution behavior and surface tension effects of organic compounds in nucleating cloud droplets. *Geophys. Res. Lett.* **1996**, *23* (3), 277−280.
(61) Petters, M. D.; Prenni, A. J.; Kreidenweis, S. M.; DeMott, P. J.; Matsunaga, A.; Lim, Y. B.; Ziemann, P. J. Chemical aging and the hydrophobic-to-hydrophilic conversion of carbonaceous aerosol. *Geophys. Res. Lett.* **2006**, *33* (24), L24806.
(62) George, I. J.; Chang, R. Y.-W.; Danov, V.; Vlasenko, A.; Abbatt, J. P. D. Modification of cloud condensation nucleus activity of organic aerosols by hydroxyl radical heterogeneous oxidation. *Atmos. Environ.* **2009**, *43* (32), 5038−5045.
(63) Smith, J. D.; Kroll, J. H.; Cappa, C. D.; Che, D. L.; Liu, C. L.; Ahmed, M.; Leone, S. R.; Worsnop, D. R.; Wilson, K. R. The heterogeneous reaction of hydroxyl radicals with sub-micron squalane particles: A model system for understanding the oxidative aging of ambient aerosols. *Atmos. Chem. Phys.* **2009**, *9* (9), 3209−3222.
(64) Heald, C. L.; Kroll, J. H.; Jimenez, J. L.; Docherty, K. S.; DeCarlo, P. F.; Aiken, A. C.; Chen, Q.; Martin, S. T.; Farmer, D. K.; Artaxo, P. A simplified description of the evolution of organic aerosol composition in the atmosphere. *Geophys. Res. Lett.* **2010**, *37* (8), L08803.
(65) Russell, L. M.; Bahadur, R.; Ziemann, P. J. Identifying organic aerosol sources by comparing functional group composition in chamber and atmospheric particles. *Proc. Natl. Acad. Sci. U.S.A.* **2011**, *108* (9), 3516−3521.
(66) Hu, K. S.; Darer, A. I.; Elrod, M. J. Thermodynamics and kinetics of the hydrolysis of atmospherically relevant organonitrates and organosulfates. *Atmos. Chem. Phys.* **2011**, *11* (16), 8307−8320.
(67) Liu, S.; Shilling, J. E.; Song, C.; Hiranuma, N.; Zaveri, R. A.; Russell, L. M. Hydrolysis of organonitrate functional groups in aerosol particles. *Aerosol Sci. Technol.* **2012**, *46* (12), 1359−1369.

(68) Kroll, J. H.; Smith, J. D.; Che, D. L.; Kessler, S. H.; Worsnop, D. R.; Wilson, K. R. Measurement of fragmentation and functionalization pathways in the heterogeneous oxidation of oxidized organic aerosol. *Phys. Chem. Chem. Phys.* **2009**, *11* (36), 8005−8014.
(69) Elemental composition and relevant functional groups were determined for each of the molecule structures in Tables S1−S3 of the Supporting Information; the molar volume was estimated using the method of Girolami, and intrinsic κ was computed using the ratio of molar volume of solute and solvent:[51] Girolami, G. S. A simple "back of the envelope" method for estimating the densities and molecular volumes of liquids and solids. *J. Chem. Educ.* **1994**, *71* (11), 962−964.
(70) Except for short chain dicarboxylic acids, most organic acids are in the sparingly soluble regime. See Table 3 of the following reference for a contrast of solubility-limited and nonsolubility-limited activation diameters for 19 organic acids: Huff Hartz, K. E. H.; Tischuk, J. E.; Chan, M. N.; Chan, C. K.; Donahue, N. M.; Pandis, S. N. Cloud condensation nuclei activation of limited solubility organic aerosol. *Atmos. Environ.* **2006**, *40* (4), 605−617.